Pressure Swing Adsorption: Effects of Incomplete Purge

Theoretical and experimental studies of pressure swing adsorption (PSA) cycles for various extents of purging have been conducted. In both the theoretical and experimental portions, pressurization was accomplished with product rather than with feed. A simple, local equilibrium model was employed, and the results were analyzed by the method of characteristics. It was found that for difficult separations (i.e., closely spaced isotherms and/or heavily contaminated feeds), incomplete purging, e.g., as little as 50% complete, yielded recoveries attainable only at much higher pressure ratios with complete purge. Conversely, for easy separations (i.e., widely spaced isotherms and dilutely contaminated feeds), incomplete purging was less attractive, yielding only slight improvement over complete purge.

Splitting oxygen from air with zeolite 5A is moderately difficult due to the proximity of the isotherms and due to the predominance of the more strongly adsorbed nitrogen in the feed. This case was also modeled and was studied experimentally. The experiments yielded nearly double the recovery of oxygen for minimal purge compared with that available with complete purge. The productivity of oxygen was relatively high, e.g., 0.0378 $m^3(O_2$ at STP)/kg (adsorbent) · h. Those experiments validated the trends predicted theoretically.

Michael J. Matz, Kent S. Knaebel
Department of Chemical Engineering
Ohio State University
Columbus, OH 43210

Introduction

The conventional four-step PSA cycle that separates a binary mixture is comprised of feed, blowdown, purge, and pressurization, as shown in Figure 1. Each of these steps is thought to serve a concise and vital function that enables successful operation of the PSA system. In this study, the extent of completion of the purge step is considered. Since the feed and purge steps are usually countercurrent, incomplete purge results in a composition tail containing some of the more strongly adsorbed component at the feed end of the column. Pressurization with pure product pushes that residual material into a smaller section of the adsorbent bed closer to the feed end, as shown in Figure 2. The presence of the compressed tail reduces the quantity of both the feed that can be accomodated prior to breakthrough and the gross product obtained. Generally, if the amount of pure product saved by incomplete purge exceeds that lost by reducing the feed, an increase in recovery is possible.

This type of operation has been common in industrial practice, as recognized by Wagner (1969) and Wankat (1986). Previous research on this subject has been primarily concerned with overall operating performance. For example, Sircar and Kumar (1985) developed an equilibrium theory to analyze the desorption behavior for binary gas mixtures. Light-product purity and proper purge-to-feed ratio have been considered by Yang and Doong (1985), Doong and Yang (1986), and Yang (1987). An implication of their results is that it is not feasible to maintain high product purity while increasing recovery by decreasing the purge-to-feed ratio. Kirkby and Kenney (1987) developed a cell model and performed experiments that suggested that an optimum purge amount exists for which product purity and recovery are maximized. Their model indicated that the optimum occurs when the purge gas profile breaks through, i.e., at complete purge. Their experiments, however, revealed that a lesser amount was optimal.

In summary, the previous papers on this subject have dealt with practical aspects related to operating conditions, and they have focused their conclusions on effects of extent of purge on performance. They have not generally interpreted the phenom-

---

Correspondence concerning this paper should be addressed to K. S. Knaebel.

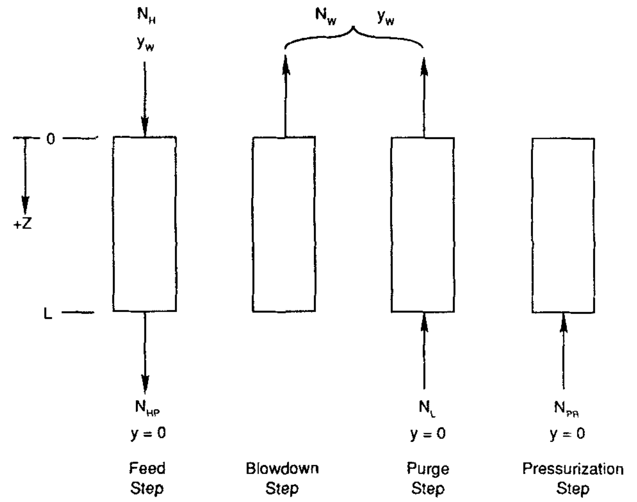

Figure 1. Column orientation and flow directions during the four actual steps of a typical PSA cycle.

ena in terms of wave movements, however. That is, the relationship between the residual impurity and the formation and propagation of a shock front has not been discussed. Furthermore, it is unclear in those previous studies, whether the simple wave nature of the purge step was understood or accepted. Accordingly, the relevant PSA steps have been evaluated here in terms of their wave-like characteristics. A simple theoretical analysis has been performed, and experiments have been conducted to validate those results.

Theory

This study considers a binary feed of arbitrary composition in which both components adsorb with linear isotherms. Therefore, the theory of Knaebel and Hill (1985) is used as the basis of the present model. That theory is based on local equilibrium, ignoring all dissipative effects, such as intraparticle diffusion, axial dispersion, and pressure drop along the axis of the bed. To conserve space, the remaining assumptions and basic equations employed there are not repeated here; only the pertinent results have been extracted.

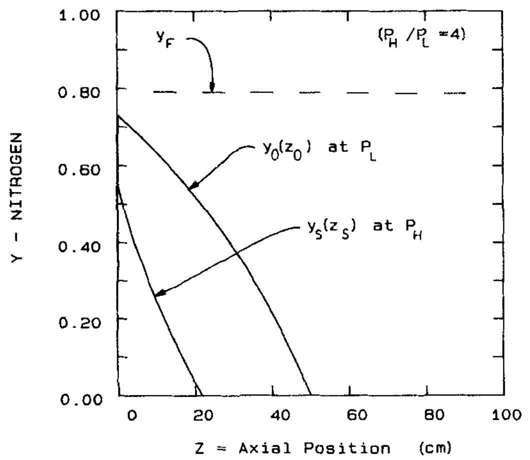

Figure 2. Predicted axial composition profiles following the purge and pressurization steps.

Conditions shown are for $\Psi = 4$, $\beta = 0.6$, and $y_F = 0.79$.

Since the purge step is accomplished with recycled pure product, a simple wave is generated within the adsorbent bed. This wave spreads as it propagates over the length of the column. Ultimately, the composition profile obtained at the end of the purge step is analogous to that shown in Figure 2. The extent of purge is considered as a fraction of complete purge, expressed as

$$X = \beta_A u_L t_L / L = N_{PU}/N^*_{PU} \tag{1}$$

where $N^*_{PU} = \phi = (\epsilon A_{cs} L P_L)/(\beta_A R T)$ is the moles required for complete purge, as given by Knaebel and Hill (1985). The characteristic relation, which defines the propagation rate of material at a certain composition, that holds during the purge step is

$$u_{y_0} = \frac{\beta_A u_L}{[1 + (\beta - 1) y_0]^2} = \left.\frac{\Delta z}{\Delta t}\right|_{y_0} = \frac{z_0 - L}{t_L} \tag{2}$$

where y_0 is an arbitrary mole fraction of the more strongly adsorbed component. This expression, therefore, defines the simple wave that is generated during the purge step. Note that the velocities with respect to z-t coordinates are inherently negative. The parameters β_A and β relate to adsorbent/adsorbate properties, i.e., $\beta = \beta_A/\beta_B$ and $\beta_j = 1/(1 + (1 - \epsilon/\epsilon)\, k_j)$ where ϵ is the adsorbent bed porosity and k_j is the slope of the isotherm of component j. Refer to Figures 1 and 3 for the direction convention and connotations of the variables.

During the pressurization step, two relations govern the composition shift and position shift, respectively:

$$\frac{y_S}{y_0} = \left(\frac{1 - y_S}{1 - y_0}\right)^{\beta} \Psi^{\beta - 1} \tag{3}$$

$$\frac{z_S}{z_0} = \left(\frac{y_S}{y_0}\right)^{\beta/1-\beta} \left(\frac{1 - y_0}{1 - y_S}\right)^{1/1-\beta} \left(\frac{1 + (\beta - 1) y_S}{1 + (\beta - 1) y_0}\right) \tag{4}$$

where $\Psi = P_H/P_L$. Finally, during the feed step the characteristic velocity is

$$u_{y_S} = \frac{\beta_A u_H [1 + (\beta - 1) y_F]}{[1 + (\beta - 1) y_S]^2} = \left.\frac{\Delta z}{\Delta t}\right|_{y_S} = \frac{z - z_S}{t} \tag{5}$$

Before further considering PSA performance, it is appropri-

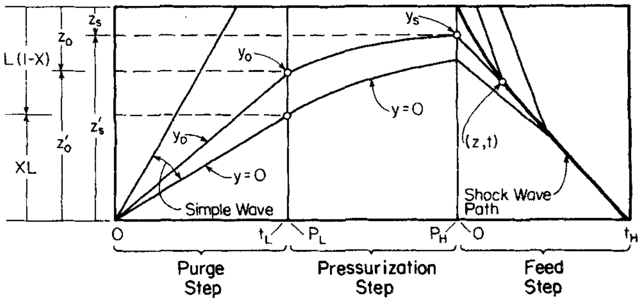

Figure 3. Characteristics describing the path of composition y_0, which results from the simple wave of the purge step.

The path can be followed as its composition shifts due to pressurization to y_S, and as it is incorporated into the shock wave at (z, t) during the feed step.

ate to consider the potential origin of multiple shock fronts during the feed step. Since the composition profile at the beginning of the feed step is complicated, as shown in Figure 2, it is conceivable that variations of composition and velocity, along with the differing adsorption selectivities of the components, could lead to the formation of multiple shock fronts. If that were the case, column behavior would be difficult to understand and analyze. The method of characteristics, however, provides a means by which the formation of a shock wave can be predicted and, subsequently, the trajectory can be determined. This subject is described in more detail in the appendix. The conclusion reached there is that multiple shock waves are not, in fact, anticipated at conditions typically encountered in PSA cycles, despite the presence of complicated column composition profiles.

Consequently, it is possible to analyze the feed step of a PSA cycle by considering the propagation of a single shock wave. To do so, it is helpful to imagine a point in its path (z, t), as shown in Figure 3. The characteristics that intersect at that point have compositions $y(z_S, z, t)$ and y_F, at the leading and trailing edges, respectively. The former represents the unique characteristic that originates at $(z_S, t = 0)$. Actually, that composition and initial position are determined during the purge step and are affected by the pressurization step, as also is illustrated in Figure 3.

In view of that, it is possible to discern the composition at the leading edge of the shock wave by solving the preceding system of equations, e.g., by combining Eqs. 5, 4 and 2, respectively, as follows

$$y_S = f(y_0, y_S, z, t) \tag{6}$$

Thus, Eqs. 3 and 6 comprise a pair of nonlinear equations that can be solved, in principle, for y_S and y_0 given z, t, Ψ and the other relevant parameters.

The path of the shock wave, which leads to the point (z, t), is given by

$$u_{SH} = \left.\frac{dz}{dt}\right|_{SH} = \frac{\beta_A u_H}{1 + (\beta - 1) y_S} \tag{7}$$

Since the composition at the leading edge of the shock wave, y_S, varies nonlinearly along the shock path, it is not usually possible to determine the path analytically. Furthermore, the column length is generally explicitly defined (rather than the feed step time) so it is convenient to integrate the inverse of Eq. 7, e.g., by a Runge-Kutta technique, to the point at which $z = L$, or $y_S = 0$, which ever occurs first. In the latter case, the remaining time for the shock wave to reach the end of the adsorbent bed is trivial to evaluate.

As mentioned previously, the analysis is restricted to cases in which the compressed simple wave is overtaken (so that $y_S = 0$) in conjunction with 100% utilization of the adsorbent bed. Those restrictions have eliminated the necessity of considering a complicated blowdown step, and have permitted a simpler analysis of the purge and pressurization steps. The ultimate composition of the material in the column following blowdown is determined by following the pressure change along a characteristic as in Eqs. 3 and 4. The ultimate value of y is y_W, i.e., after the pressure shift is complete. At that point $\Psi = P_L/P_H$.

Since the composition, y_w, reached during blowdown reverts to the feed composition during the pressurization step, it will rarely be practicable to allow any of the composition plateau represented by y_w to remain in the bed. The presence of such a plateau would make that portion of the bed useless and would probably preclude production of pure product. Therefore, only a tail of the simple wave can be allowed to remain in the column without adversely affecting performance.

Ultimately, the recovery of pure product can be predicted by relations presented previously (Knaebel and Hill, 1985) incorporating the foregoing analysis of incomplete purge. The effect on recovery of extent of purge, feed composition, adsorbent selectivity, and pressure ratio have been studied and will be discussed later.

Experimental Methods

The purpose of this portion of the study was to validate the foregoing model and to assess aspects of the purge step that may not have been taken into account by the model. Six experiments were performed using different amounts of purge in each. Overall performance, in terms of recovery of pure product was the focal point of this portion of the research, but the effect of incomplete purging on product purity was also of concern.

The four step PSA cycle shown in Figure 1 with pressurization by product was employed. The apparatus flowsheet is shown in Figure 4, though the data acquisition system has been omitted. Only one column was operated so that the attainable cyclic steady state was representative of one fractional purge condition. While two column operation was possible, it was decided that a small difference in capacity between the columns would have led to different extents of purge during the same experiment, which may have produced confusing results.

Room air, which had passed through a guard bed of 5A molecular sieve adsorbent to remove water vapor and CO_2, was compressed into the feed tank, then delivered to the column during the feed step. The column was uninsulated and exposed to ambient air.

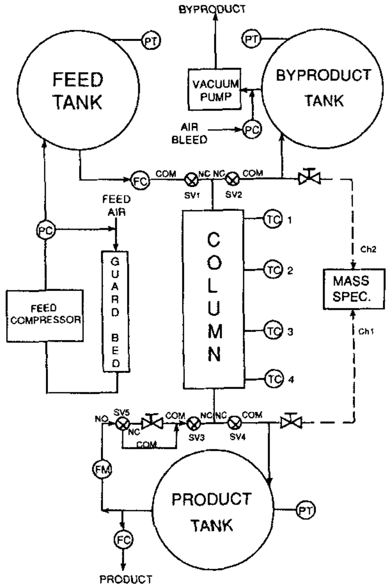

Figure 4. Experimental PSA apparatus and instruments.

Values were manipulated by and all temperatures, flow rates, pressures and compositions were recorded by a microcomputer-based data acquisition and control system.

Four thermocouples (Omega Engineering, 1.59 mm diameter, K-type, exposed junction) were also inserted in the column, at spacings of 0.1778 m. Temperature rises at each thermocouple were used to estimate the propagation rate of this wave and to control the feed step duration, as described elsewhere (Matz and Knaebel, 1987). A Digital Equipment Company Micro PDP-11/73 microcomputer with ancillary interface boards was used to accumulate the data and to switch the solenoid valves synchronously.

Following the feed step, the column underwent blowdown into a surge tank which was maintained at subatmospheric pressure by a vacuum pump. Essentially nitrogen-free oxygen and argon (usually about 94% and 5%, respectively), obtained during the feed step and received by the product tank, was then used to purge the column. A metering valve controlled the purge flow rate in the critical flow regime, assuring constant flow. The same flow rate was used in all of the incomplete purge experiments, but the duration of the purge step was varied.

Pressurization with product returned the column to the high pressure level at which feed occurred. Also, a mass flow controller allowed continuous product release while a mass spectrometer (Perkin-Elmer, MGA 1200) monitored product composition, as well as the effluent streams during feed, blowdown, and purge steps. The feed step was always allotted 100 s, and the blowdown step always lasted for 30 s. The purge step varied between 0 and 60 s. Pressurization actually required less than 10 s, though as much as 70 s was allowed; the excess permitted constant total cycle times among the experiments. After operating the PSA system in that manner for several hours (and hundreds of cycles), cyclic steady state was reached and data of two typical sequential cycles were recorded. Table 1 lists the column dimensions and adsorbent properties and Table 2 lists the conditions and overall results of all six experiments.

Results and Discussion

Since the shock wave that was observed experimentally was not perfect, it was not possible to use 100% of the adsorbent bed during the feed step. As a result, the feed step was terminated at incipient breakthrough leaving a small portion of pure product in the bed. Thus, the column was not fully utilized during the feed step and it was partially purged (by the expanding retained product) during the blowdown step. Both of these effects could have been taken into account by the same methods of analysis. Nevertheless, to avoid the potentially confusing interactions of analyzing incomplete feed with incomplete purge, it has been presumed that the feed step is complete. Furthermore, the results of the theoretical analysis are based on a known minimum extent of purge. This quantity is established by the characteristic that intersects the exit of the bed at the end of the purge step. Although this characteristic does not move during the pressurization step, its corresponding composition changes according to Eq. 3. The ultimate composition must be less than that of the feed. Hence, the composition prior to pressurization may be determined, and Eq. 2 may be used to determine the minimum extent of purge for the respective conditions.

Table 1. Column Dimensions and Adsorbent Properties

Column length	0.711 m
Inner diameter	0.021 m
Mass of adsorbent	0.184 kg
Adsorbent density	1,552. kg/m^3
Bulk adsorbent density	733. kg/m^3
Adsorbent porosity	0.528

Theory

Accordingly, it is possible to simulate PSA cycles for a range of feed compositions, pressure ratios, adsorbent selectivities, and extents of purge. Figures 5 and 6 show the results of several such case studies. Figure 5 applies for cases in which adsorbent selectivity is high ($\beta = 0.1$). Reduction of the purge amount from the complete value yields little improvement in recovery for feed dilutely contaminated with the more strongly adsorbed component ($y_F = 0.1$). For example, at a pressure ratio of 2 and 90% complete purge, the recovery is improved only by about 10% over that for complete purge. Conversely, when a majority of the feed is comprised of the more strongly adsorbed component ($y_F = 0.9$), substantial improvement of product recovery is possible. Positive recovery is possible only at pressure ratios above 10 for complete purge, but by purging as little as 50% it is possible to attain positive recoveries above a pressure ratio of 5. Furthermore, at a pressure ratio of 10 and 50% purge, it is possible to achieve 50% recovery. At higher pressure ratios, however, the advantages of partial purge diminish.

The last set of conditions considered is the situation of low adsorbent selectivity and heavily contaminated feed. In that regard, Figure 6 demonstrates that significant improvements are again possible, for $\beta = 0.9$ and $y_F = 0.9$. In particular, at complete purge positive recoveries are again attained only at pressure ratios above 10. In contrast, reduction of the amount of purge by only 10% permits positive recoveries at pressure ratios above about 2. Furthermore, at the same fractional purge and a pressure ratio of 10 it is possible to reach roughly 8% recovery, which is only achievable at a pressure ratio of 100 when complete purge is used.

To conclude the discussion of the theoretical predictions, it is appropriate to mention that, in the previously discussed cases as well as others that were not reported in detail, incomplete purge does not generally allow an improvement of recovery over that ultimately attainable with complete purge, i.e., at very high pressure ratios. Conversely, it permits equivalent recoveries at lower pressure ratios.

Experiments

This section describes experimental measurements of effluent composition histories, shock wave and simple wave propagation rates, and overall performance (in terms of product recovery). Figure 7 displays the instantaneous effluent compositions during feed, blowdown, and purge steps from three experiments. For comparison, the theoretical values (based on 100% utilization of the bed during the feed step) are also shown.

The simple wave, represented by the effluent composition history of the purge step, always followed a similar path. Each profile was terminated at the onset of the pressurization step. All of the experimental profiles reflect the inability to attain complete saturation of the bed. This resulted from the S-shaped breakthrough curve, of which only the tip was permitted to reach the end of the bed. This deviated from the square-wave breakthrough anticipated by the theory, and contributed to inadvertent partial purging of the bed during the blowdown step. Differences between the individual profiles appear to stem from

Table 2. PSA Experimental Conditions and Performance

	Experiment Number					
	1	2	3	4	5	6
$\overline{P}_H$ (bar)	3.425	3.471	3.475	3.506	3.486	3.479
$\overline{P}_L$ (bar)	0.188	0.192	0.193	0.199	0.201	0.199
$\Psi = P_H/P_L$	18.2	18.1	18.0	17.7	17.3	17.5
$\overline{Q}_H$($\times 10^{-3}$ mol/s)	2.266	2.078	2.184	2.073	2.021	1.957
$\overline{Q}_{HP}$($\times 10^{-3}$ mol/s)	5.429	5.429	6.768	8.032	8.627	9.073
Room Temp. (K)	299.0	298.9	299.0	299.2	297.8	298.2
y_{A_F}	0.783	0.783	0.783	0.783	0.783	0.783
X = Fraction purged at 0.0915 mol/s	1.00	0.75	0.50	0.25	0.10	0.00
$(1 - y_A)_{HP}$	0.989	0.989	0.990	0.990	0.983	0.982
R_{exp}	0.218	0.240	0.283	0.354	0.387	0.419
Productivity m^3 (O$_2$ at STP/kg (adsorbent) · h	0.0227	0.0230	0.0285	0.0338	0.0360	0.0378

changes in the ultimate composition achieved during blowdown. The compositions measured by the mass spectrometer may have been erroneous due to its sensitivity to variations of the sampled gas pressure. Dead volume (between the end of the bed and the sampling port) and other distance-velocity lags may also have distorted the composition histories in these experiments.

The instantaneous high pressure product composition history was also measured. Only during the cycle in which no purge was used does the composition appear to deviate from being nearly nitrogen-free. The absence of nitrogen in the product resulted from the fact that breakthrough was not achieved, i.e., the bed was not 100% utilized. Consequently, a lower ultimate blowdown composition within the bed is achieved, and a cleaner bed is established following purge and pressurization.

To assess the degree of agreement between theory and experiments, a graphical comparison of predicted recoveries (for different adsorbent selectivities) and those that were experimentally measured is shown in Figure 8. Due to inadequacies of the experimental equipment, which have been discussed previously, it was not possible to reach perfect correspondence between the experimental conditions and those taken into account by the theory. Despite that, the trend of increasing recovery for decreasing extent of purge is evident in both theory and experiments. In addition, it is clear that the experimental performance roughly corresponded to that predicted for an adsorbent selectivity given by $\beta \approx 0.7$. A final basis of comparison is the productivity, values for which are listed in Table 2. The trend is that the productivity increases from 0.023 to 0.038 m^3 (O$_2$ at STP)/kg(adsorbent) · h as the fraction purged decreases from 1.0 to 0.0. The effect is due to increasing recovery, as the amount of feed expressed on the same basis actually decreases. The values are larger than those obtained in earlier experiments (Kayser and Knaebel, 1986) and are larger than for a commercial oxygen PSA system (Yang, 1987).

Conclusions

A simple mathematical model of equilibrium-based pressure swing adsorption has been adapted to a cycle in which the purge step is incomplete. That model portrays the movement of material in the adsorbent bed as waves, taking into account pressure variation with time, velocity variation with composition, and composition variations over the entire range encompassed by a binary mixture. Those wave movements are subsequently employed to establish step times and material balances. The benefit of such concepts is that they help elucidate the effects on performance of subtle changes in operating conditions, such as incomplete purge.

Experiments were conducted that sought similar insight to performance through observation of wave movements. These

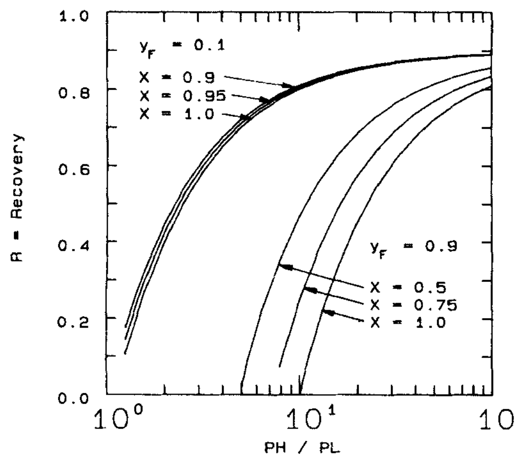

Figure 5. Recovery as a function of pressure ratio for various values of extent of purge, *X*.
Conditions are for $\beta = 0.1$ and $y_F = 0.1$ or $y_F = 0.9$.

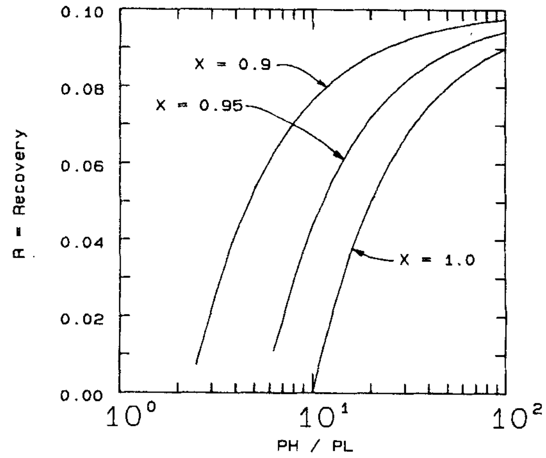

Figure 6. Recovery as a function of pressure ratio for various values of extent of purge, *X*.
Conditions are for $\beta = 0.9$ and $y_F = 0.9$.

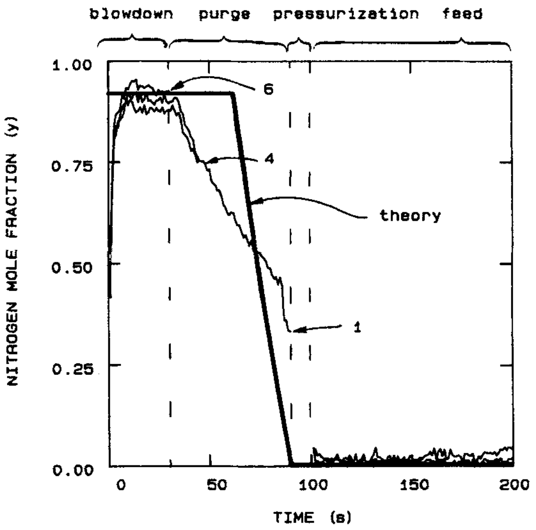

Figure 7. Composition-time histories for experiments 1, 4 and 6 (identified by the same number). The column effluent streams from the blowdown, purge and feed steps are shown.

goals were achieved by monitoring composition of all streams during the PSA cycle, and by observing the thermal wave propagation through the adsorbent bed during the feed step. This approach permitted direct analysis of incomplete purge without resorting to a rather vague purge-to-feed ratio. As a result, one previously held notion, that product quality must deteriorate as the purge-to-feed ratio decreases, has been shown to be not generally true.

The theory asserts and the experiments demonstrate that high purity can be maintained even at low extents of purge. Furthermore, significant increases in recovery of that pure product are possible at reduced purge levels when the pressure ratio is specified. In particular, it appears that the beneficial effects of incomplete purge are most significant for situations in which the separation would appear difficult, i.e., for feeds that are heavily contaminated with the more strongly adsorbed component and/or for low adsorbent selectivities.

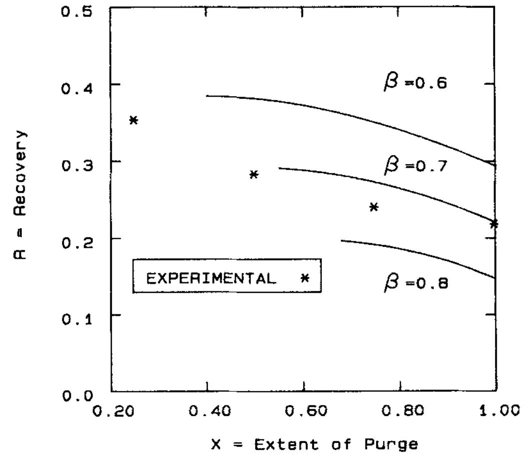

Figure 8. Recovery of oxygen and argon from air with 5A zeolite at 298 K.

Experimental values and predictions for various values of β, for $\Psi = 18$ and $y_F = 0.79$.

The inducement for developing the model and for conducting the experiments was to elucidate trends while maintaining simplicity. The primary inadequacies of the present model are the limited range of applicability due to the assumptions of linear isotherms and isothermal conditions. These may not be unduly harsh because they correspond to conditions that enhance PSA performance. Furthermore, the experiments presented here and those conducted earlier (Kayser and Knaebel, 1986; Matz and Knaebel, 1987) imply that temperature swings of 20 to 30 K and slight curvature of the isotherms do not adversely affect the predictions.

Acknowledgment

This research was partially sponsored by the Air Force Office of Scientific Research/AFSC, United States Air Force, under contract. The United States Government is authorized to reproduce and distribute reprints for governmental purposes notwithstanding any copyright notation hereon. The instruments were provided in part by funds from NSF Grant Number CPE-8405892. The authors are grateful to Union Carbide Corporation for donation of the adsorbent used in this study.

Notation

A_{CS} = cross-sectional area
k_j = equilibrium isotherm distribution coefficient
L = absorbent bed length
N = moles
P = absolute pressure
Q = molar flow rate
R = gas constant
T = absolute temperature
t = time
u = interstitial velocity
X = fraction of partial purge
y = mole fraction of component A (more strongly adsorbed)
z = axial position
z' = axial position measured in opposite direction to z

Greek letters

$\beta = \beta_A/\beta_B$
$\beta_j = 1/(1 + (1 - \epsilon/\epsilon)k_j)$
ϵ = bed void fraction
$\gamma = 1 + (\beta - 1)y$
Δ = axial position increment
$\phi = \epsilon A_{CS} L P_L / \beta_A R T$
$\sigma = 1/u_y$
Ψ = pressure ratio = $P_{\text{final}}/P_{\text{initial}}$

Subscripts

A = more strongly adsorbed component
B = less strongly adsorbed component
exp = experimental
F = feed
H = refers to feed step
HP = refers to product of feed step
i = refers to an axial position
j = refers to a species
L = refers to purge step
O = condition following the purge step
PR = refers to pressurization
PU = refers to purge
PU^* = refers to complete purge
S = condition following the pressurization step
SH = refers to shock wave
W = refers to blowdown or exhaust

Literature Cited

Cen, P., and R. T. Yang, "Bulk Gas Separation by Pressure Swing Adsorption," *Ind. Eng. Chem. Fund.*, **25,** 758 (1986).

Doong, S. J., and R. T. Yang, "Parametric Study of the Pressure Swing Adsorption Process for Gas Separation: A Criterion for Pore Diffusion Limitation," *Chem Eng. Comm.*, **41,** 163 (1986).

Kayser, J. C., and K. S. Knaebel, "Pressure Swing Adsorption: Experimental Study on an Equilibrium Theory," *Chem. Eng. Sci.*, **41,** 2931 (1986).

Kirkby, N. F., and C. N. Kenney, "The Role of Process Steps in Pressure Swing Adsorption," *Fund. of Adsorption*, Engng. Foundation, New York, 325 (1987).

Knaebel, K. S., and F. B. Hill, "Pressure Swing Adsorption: Development of an Equilibrium Theory," *Chem. Eng. Sci.*, **40,** 2351 (1985).

Matz, M. J., and K. S. Knaebel, "Temperature Front Sensing for Feed Step Control in Pressure Swing Adsorption," *Ind. Eng. Chem. Res.*, **26,** 1638 (1987).

Rhee, H. K., R. Aris, and N. R. Amundson, *First-Order Partial Differential Equations*, **I,** Prentice-Hall, Englewood Cliffs, NJ (1986).

Sircar, S., and R. Kumar, "Equilibrium Theory for Adiabatic Desorption of Bulk Binary Gas Mixtures by Purge," *Ind. Eng. Chem. Proc. Des. Dev.*, **24,** 358 (1985).

Wagner, J. L., "Selective Adsorption Process," U.S. Patent No. 3,430,418 (1969).

Wankat, P. C., *Large Scale Adsorption and Chromatography*, **I,** CRC Press, Boca Raton, FL, 95 (1986).

Yang, R. T., *Gas Separation by Adsorption Processes*, Butterworths, Boston, 328 (1987).

Yang, R. T., and S.-J. Doong, "Gas Separation by Pressure Swing Adsorption: A Pore Diffusion Model for Bulk Separation," *AIChE J.*, **31,** 1829 (1985).

Appendix

The envelope for the formation of a shock wave can be determined for a variety of initial and boundary conditions. Rhee et al. (1986) have suggested procedures that apply for the case of constant velocity. Those are extended here to the case of variable velocity. The boundary and initial conditions applicable to the feed step, in a PSA cycle with incomplete purge followed by pressurization with product, are:

$$\begin{array}{lll} \text{At } t = 0, & z^* \geq z \geq 0 & y = F(z) \\ \text{At } t = 0, & L \geq z \geq z^* & y = 0 \\ \text{At } t \geq 0 & z = L & y = y_F \end{array}$$

These are shown schematically in Figures 2 and 3.

The characteristic velocity is (Knaebel and Hill, 1985):

$$u_y = \left.\frac{dz}{dt}\right|_y = \frac{\beta_A u}{1 + (\beta - 1)y} = \frac{\beta_A u_H[1 + (\beta - 1)y_F]}{[1 + (\beta - 1)y]^2} \qquad \text{(A1)}$$

It is convenient, in light of the reciprocal dependence of velocity on composition, to employ the reciprocal velocity or "slowness," $\sigma_y = 1/u_y$.

It is assured that a shock wave will be formed at the composition discontinuity, and that that wave will propagate at a rate that depends on the composition at the leading and trailing edges of the shock. Whether or not another shock wave develops as a result of interactions of the complex initial profile may be assessed by considering the hypothetical intersection of two characteristics at (z', t'). If the characteristics arise from the $t = 0$ axis at z_i and $z_i + \Delta z (= z_{i+\Delta})$ along the bed axis then the coordinates of the intersections are:

$$z' = z_i + \frac{\sigma_{i+\Delta}}{\sigma_{i+\Delta} - \sigma_i} \Delta z \qquad \text{(A2)}$$

$$t' = \frac{\sigma_i \sigma_{i+\Delta} \Delta z}{\sigma_{i+\Delta} - \sigma_i} \qquad \text{(A3)}$$

The interval, Δz, may be allowed to shrink to a differential length, which in turn leads to the differential version of the preceding equations. The origin of the shock occurs at the minimum value of time at which characteristics intersect.

$$\frac{dt'}{dz} = \frac{dt'}{dy}\frac{dy}{dz} = 2\sigma + \sigma^2 \frac{dy}{dz}\frac{d}{dy}\left[\frac{dz}{dy}\frac{dy}{d\sigma}\right] = 0 \qquad \text{(A4)}$$

Inserting the definition of slowness from above yields

$$2\gamma^2 + \frac{\gamma^4}{2(1 - \beta)^2} \ln \gamma + \frac{\gamma^3}{2(\beta - 1)} \frac{dy}{dz}\frac{d^2 z}{dy^2} = 0 \qquad \text{(A5)}$$

where: $\gamma = 1 + (\beta - 1)y$.

Values that are typical of PSA operation with a simple four step cycle have been tested with Eq. A5 and it has been found that only a single shock wave is formed. It corresponds to the discontinuity between the feed composition and that of the initial contents of the column at the feed end. It is expected, however, that more sophisticated steps or processes involving multicomponent mixtures will generate more complicated wave phenomena.

Manuscript received Dec. 8, 1987, and revision received Apr. 11, 1988.